Simulation of Deep Eutectic Solvents: Progress to Promises

Caroline Velez and Orlando Acevedo*

Department of Chemistry, University of Miami, Coral Gables, Florida 33146

E-mail: orlando.acevedo@miami.edu

ADVANCED REVIEW

ABSTRACT: Deep eutectic solvents (DESs) are binary or ternary mixtures of compounds that possess significant melting point depressions relative to the pure isolated components. The discovery of DESs has been a major breakthrough with multiple fields benefitting from their low cost and tunable physiochemical properties. However, tailoring DESs for specific applications through their practically unlimited synthetic combinations can be as much a hindrance as a benefit given the expense and time-required to perform large-scale experimental measurements. This emphasizes the need for fast computational tools capable of making accurate predictions of DES physiochemical properties exclusively from molecular structure. Yet, these systems are not trivial to model or simulate at the atomic level given their exceedingly non-ideal behaviors, asymmetry of components, and the complexity of their molecular electrostatic interactions. Despite the challenge, computational reports featuring quantum mechanical (QM) methods have provided significant understanding into the relationship between the melting point depression and the unique and complex hydrogen bond network present in DESs. Classical molecular dynamics (MD) methods have examined bulk-phase solvent organization in conjunction with thermodynamic and transport properties. Machine learning (ML) algorithms have shown great potential as structure-property prediction tools. Overall, this review highlights computational accomplishments that have

meaningfully advanced our understanding of DESs and strives to give the reader a sense of the overall strengths and drawbacks of the methodologies employed while hinting at promises of advances to come.

KEYWORDS: deep eutectic solvents, molecular simulation, force field, quantum mechanics, machine learning

GRAPHICAL ABSTRACT:

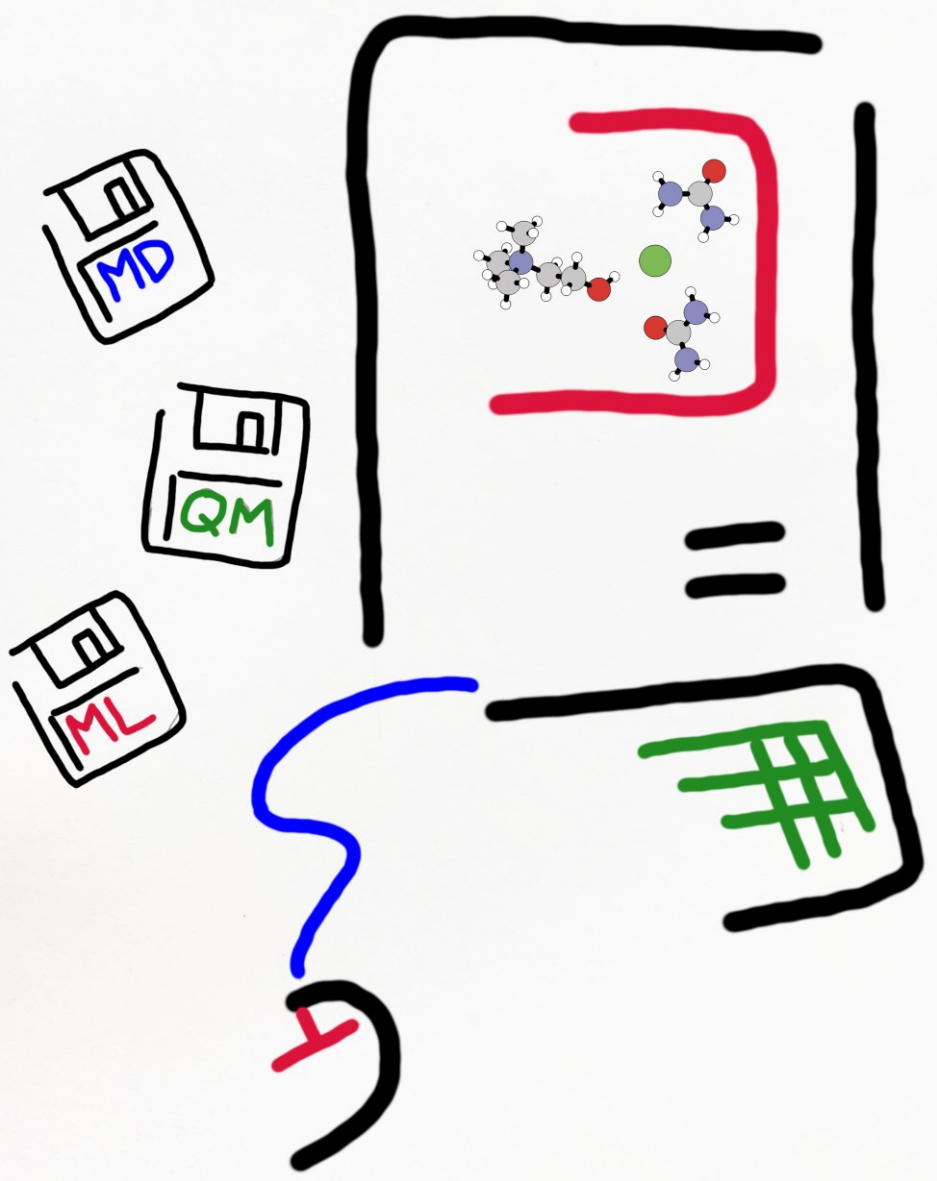

This review highlights computational accomplishments that have meaningfully advanced our understanding of deep eutectic solvents (DESs).

1. INTRODUCTION

The utilization of conventional organic solvents in chemical applications is often energy-intensive, produces environmental and health hazards, and requires expensive chemical waste disposal.[1, 2] Consequently, developing green and sustainable solvents is of the utmost importance.[3-8] The discovery of deep eutectic solvents (DESs) has been a major breakthrough in this respect with research efforts over the past twenty years directed towards elucidating the structure-property relationship of these solvents in diverse applications.[9-14] The term “deep eutectic solvent” has become a catch-all phrase that describes binary or ternary mixtures of compounds which decrease in melting temperature relative to the melting temperatures of the pure isolated components. Hence, the *eutectic temperature* is defined as the lowest melting temperature for a given mixture (with most DESs <150 ºC) and the corresponding composition is called the *eutectic composition*.[15] Deep eutectic solvents are generally composed of a hydrogen bond acceptor (HBA) such as a quaternary ammonium salt and a neutral hydrogen bond donor (HBD) that can form a complex with the halide (Figure 1).[16] Accordingly, DES physicochemical properties are primarily dependent upon the intermolecular interactions maintained by its components.[17] Capitalizing on their facile synthesis and purification process, favorable physical properties that include low vapor pressures, nonflammability, high biodegradability, and their 100% atom utilization rate,[18] deep eutectic solvents have been effectively adopted for use in multiple fields that include biotechnology and biocatalysis,[19, 20] materials,[21-23] polymers,[24-27], extractions and separations,[28-32] dissolution of metals,[33] carbohydrate chemistry,[34] gas solubility,[35, 36] energy and fuels,[37,

[38] biology,[39] biomass processing,[40, 41] and as a reaction medium for organic reactions.[42-44]

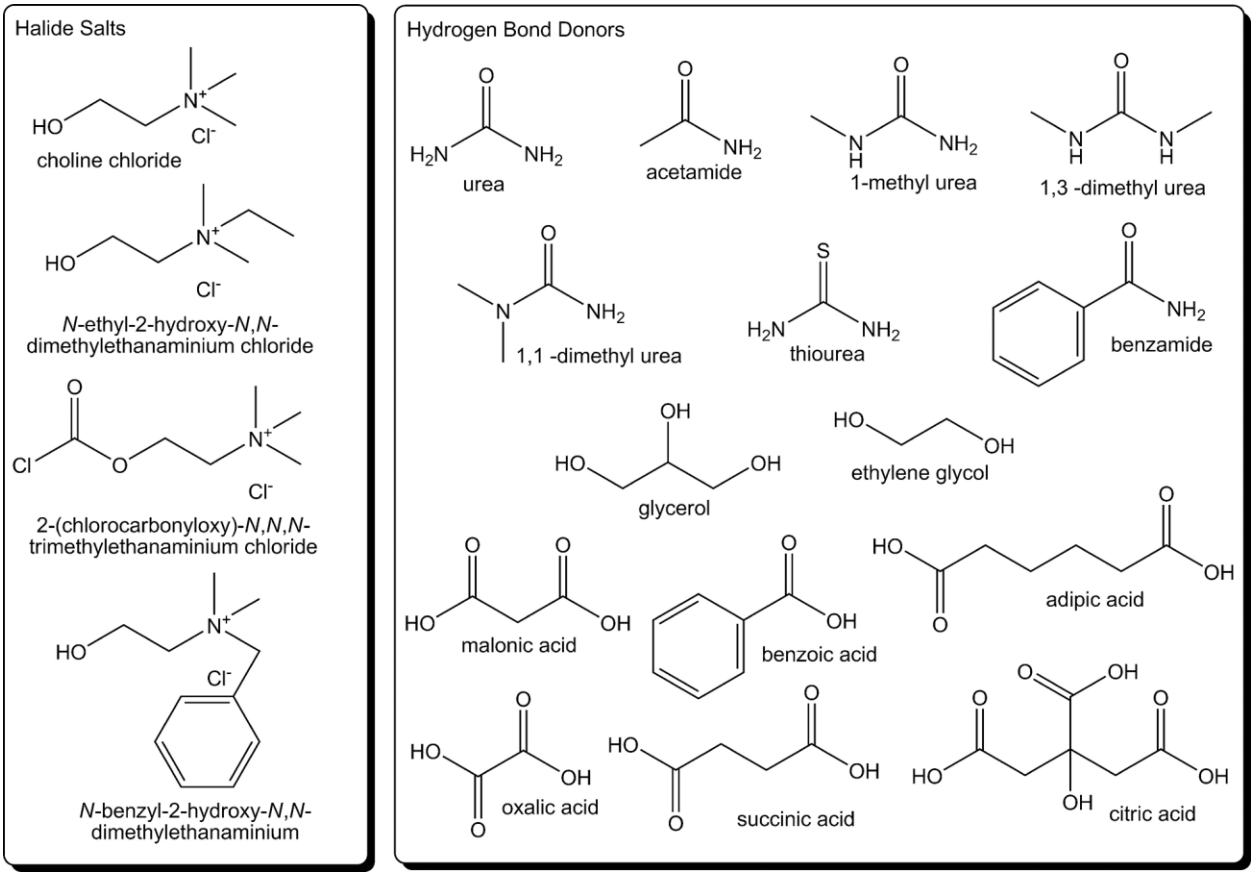

Figure 1. *Type III* deep eutectic solvent forming halide salts and hydrogen bond donors. Used with permission from E. L. Smith, A. P. Abbott, K. S. Ryder, *Chem. Rev.*, **2014**, *114*, 11060-11082**.** Deep Eutectic Solvents (DESs) and Their Applications. Copyright 2014, The American Chemical Society.

While many DES-based enhancements to chemical applications have been realized, meaningfully advancing the "designer solvent" aspect of DESs through their virtually limitless synthetic flexibility[45] can be as much a hindrance as a benefit given the expense and time-required to perform large-scale experimental measurements. The efficiency of tailoring DESs for specific purposes could be significantly improved with a

fast computational tool capable of making accurate predictions of DES physiochemical properties exclusively from its molecular structure. Yet, these systems are not trivial to model or simulate at the atomic level given their exceedingly non-ideal behaviors (in pure form or mixtures), asymmetry of components, and the complexity of their molecular electrostatic interactions.[46] This review aims to inform the reader of advancements in the development and application of theoretical and computational methods to help elucidate the molecular nature of DESs.

In Section 2, a brief background on the history, classification, and composition of DESs is provided to familiarize the reader with these unique solvent systems. Section 3 delves into research efforts that utilized quantum mechanical (QM) methods on gas phase structures and *ab initio* molecular dynamics (AIMD) on small solvent clusters. These techniques have played a significant role in elucidating the origin of DES melting point depression and the intricacies of intermolecular interactions and hydrogen bonding present in these solvents. Section 4 features an overview of molecular dynamics (MD) simulations and force field developmental efforts used to model bulk-phase DES systems with insight provided into solvent organization and thermodynamic and transport properties in pure and heterogeneous environments. Finally, Section 5 reports machine learning (ML) algorithms as property prediction tools for DESs with a brief discussion on their methodological background. Overall, this review strives to give the reader a sense of the overall performance of current simulation models and highlights the strengths and drawbacks of each method in representing the structure and properties of DESs. Given the length of this brief review, topic discussions cannot be exhaustive; however, earlier

reviews highlighting computational accomplishments are available that may fill in some of the gaps.[11, 46, 47]

2. DEEP EUTECTIC SOLVENTS

2.1 A brief history of deep eutectic solvents

The first generation of eutectic solvents included chlorometallate ionic solvents that were widely studied in the 1980s, e.g., ionic liquids (ILs) composed of $AlCl_3$ and quaternary ammonium salts.[48] In 2001, Abbott et al. built upon these previous research efforts by synthesizing a combination of metal chlorides ($ZnCl_2$, and/or $SnCl_2$) and quaternary ammonium salts in an effort to overcome limitations associated with ILs, e.g., moisture sensitivity and high cost.[49] Specifically, the mixture between choline chloride (ChCl) and zinc chloride in a 1:2 ratio provided the lowest freezing point of 23-25 °C. An abnormally deep melting point depression ($T_{eutectic}$ = 12 °C) was noted in a 2003 follow up study by the same authors for a 1:2 mole fraction ChCl:urea mixture when compared to the individual melting points of 302 and 133 °C for the isolated substrates, respectively.[16] Abbott et al. coined the term “deep eutectic solvent” to describe this observed phenomenon.[16] Looking to expand into different classes of organic molecules, DESs based on ChCl and carboxylic acids were synthesized by Abbott et al. in 2004 and were shown to exhibit a similar freezing point depression.[50] From this year onward, a steadily increasing number of DES-based research efforts were published with a major focus on understanding the physicochemical properties and thermodynamics of these solvents. DESs share similar physical properties to room temperature ionic liquids (RTILs), including high viscosity, large surface tension, low vapor pressure, and non-

flammability.[51-53] While DESs may be considered ionic liquid (IL) analogues, an important contrast is that ILs are often more expensive, nonbiodegradable, and can have high toxicities compared to the more benign nature of DESs.[54, 55] Ultimately, the most important difference between conventional ILs and DESs is that ILs are made from discrete anions and cations, whereas DESs are synthesized by mixing two components that form a eutectic mixture which typically consists of cations, anions, and neutral organic compounds.

2.2 Classification of deep eutectic solvents

Deep eutectic solvents can be classified by the general formula $Cat^{+}X^{-}zY$ where Cat^{+} represents the cation, which can be an ammonium, phosphonium, or sulfonium cation, and X^{-} is a Lewis base, typically a halide anion. The Lewis or Brønsted acid Y forms a complex anionic species with X^{-}, where z refers to the number of interacting Y molecules.[56] Based on the complexing agent, DESs are commonly divided into four types as described in Table 1.[12]

Table 1. Classification of Deep Eutectic Solvents.

Type	General formula	Terms
I	$Cat^{+}X^{-}zMCl_X$	M = Zn, Sn, Fe, Al, Ga, In
II	$Cat^{+}X^{-}zMCl_X.yH_2O$	M = Cr, Co, Cu, Ni, Fe
III	$Cat^{+}X^{-}zRZ$	Z = $CONH_2$, COOH, OH
IV	$MCl_x + RZ = MCl_{x-1}^{+}\cdot RZ + MCl_{x+1}^{-}$	M = Al, Zn and Z = $CONH_2$, OH
V	RZ	Z = thymol + menthol

Adapted with permission from E. L. Smith, A. P. Abbott, K. S. Ryder, *Chem. Rev.*, **2014**, *114*, 11060-11082**.** Deep Eutectic Solvents (DESs) and Their Applications. Copyright 2014, American Chemical Society.

Type I were the first DESs synthesized by Abbott and coworkers and are analogous to ILs formed using a metal chloride and an imidazolium or quaternary ammonium salt.[49] *Type II* DESs expanded the scope of available solvents by mixing hydrated metal halides with ChCl or a quaternary ammonium salt.[57] Abbott et al. also synthesized DESs based on quaternary ammonium salts and molecular HBDs such as amides, alcohols, and carboxylic acids (Figure 1) giving rise to the most experimentally and computationally investigated class: the *Type III* DESs.[16, 50] The use of transition metal halides such as $ZnCl_2$ with HBDs such as urea, ethylene glycol, and acetamide constitute the *Type IV* DES.[56] More recently, DESs composed of only nonionic, molecular HBAs and HBDs have been proposed as a new *Type V* class that exhibits the characteristic melting point depression arising solely from strong hydrogen bonding.[58, 59]

2.3 Composition of *Type III* deep eutectic solvents

An overwhelming majority of DES research has focused on the *Type III* class ever since Abbott et al. first reported the ChCl and urea combination dubbed “reline.”[16] Table 2 summarizes the names and compositions of the most common *Type III* DESs. With an ever-growing library of constituents estimated at 10^6–10^8 possible binary combinations,[45] many DESs have been organized into subcategories based on their behavior or nature, which include hydrophobic,[60, 61] metal-free,[62] and natural[63] DESs. The almost unlimited construction choices for *Type III* DESs allows the solvents to be particularly adaptable towards any desired application using relatively inexpensive components that possess low toxicity and high biodegradability. However, optimizing DES mixtures towards a specific application can become quickly overwhelming when using an uneducated trial-and-error approach that may easily override any potential advantages provided by the

solvent. This highlights the need for systematic studies of DESs to improve their fundamental understanding and to ultimately create predictive models.[64] As such, the present review will primarily focus on computational efforts aimed at providing predictions and insight into the structure-property relationship of *Type III* DESs.

Table 2. Deep Eutectic Solvents Composed of Choline Chloride (ChCl) and a Hydrogen Bond Donor (HBD) at Specific Ratios.

abbreviation	HBD	ChCl:HBD	name
CCEtg	ethylene glycol	1:2	ethaline
CCGly	glycerol	1:2	glyceline
CCLev	levulinic acid	1:2	
CCMal	malonic acid	1:1	maline
CCOx	oxalic acid	1:1	oxaline
CCPhe	phenol	1:2 or 1:3	
CCPro	propylene glycol	1:2	propeline
CCU	urea	1:2	reline

Adapted with permission from B. Doherty, O. Acevedo, *J. Phys. Chem. B*, **2018**, *122*, 9982-9993**.** OPLS Force Field for Choline Chloride-Based Deep Eutectic Solvents. Copyright 2018, American Chemical Society.

3. QUANTUM MECHANICS

Theoretical investigations of DESs have relied heavily on quantum mechanical (QM) modeling to help elucidate their physical, thermodynamic, and structural relationships.[47] The properties of DESs are controlled primarily by interaction energies present between the different components of the mixture (cation and anion of HBA, and the HBD species), see Figure 2;[65, 66] however, contributions from electrostatic interactions and van der Waals forces should not be discounted.[18, 67] Computational reports featuring *ab initio* based methods have largely focused on understanding the relationship between

the melting point depression and solvent organization with a strong emphasis on the unique and complex hydrogen bond network present in DESs. Further discussion and highlights are provided below.

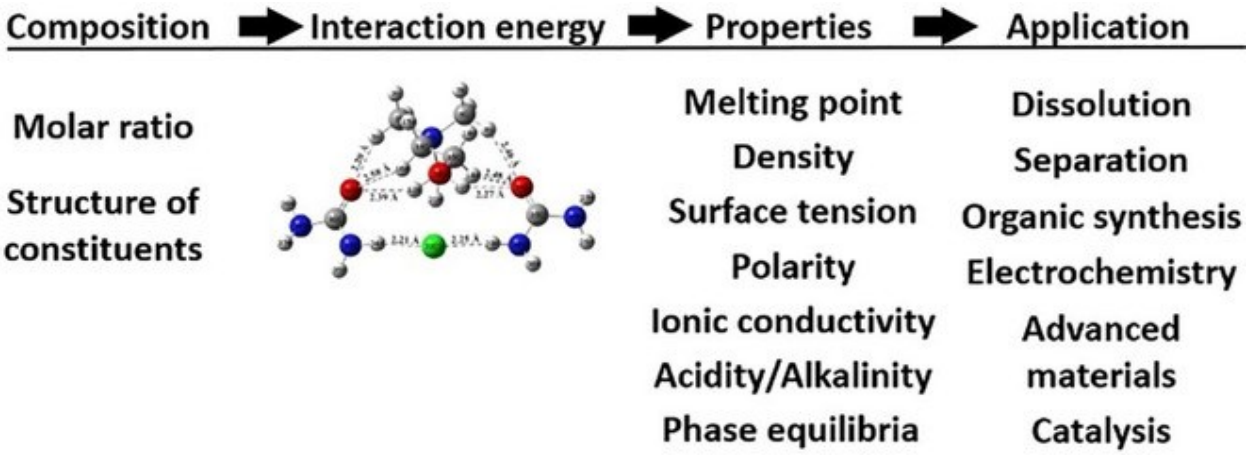

Figure 2. The relationship between structure, physical properties, and applications for deep eutectic solvents. Used with permission from A. Kovács, E. C. Neyts, I. Cornet, M. Wijnants, P. Billen, *ChemSusChem* **2020**, *13*, 3789-3804. Modeling the Physicochemical Properties of Natural Deep Eutectic Solvents. Copyright 2020, Chemistry Europe.

3.1 Melting point depression

3.1.1. Origin of decreased melting point in DESs

The origin of the characteristic DES melting point depression has been explored quite extensively by applying QM methods to small gas-phase structures and clusters. Early experimental and simulation studies postulated that negative charge delocalization may play a major role in decreasing the melting point of the individual components, a result of hydrogen bonding between the mixture components, particularly between the

halide ion and the HBD moiety.[17, 27] García et al. supported this correlation with B3LYP-D2/6-31+G(d,p) calculations and an atoms in molecules (AIM)[68] topological analysis of electron density for a set of 45 small DES clusters based on ChCl and tetraalkylammonium salts.[69] The authors noted the formation of cage-like structures with a linear relationship observed between low electron densities and low melting point depressions that arose from large charge delocalization.[69] Wagle et al. followed up the work with geometry optimizations and a charge decomposition analysis (CDA) of small ChCl-based DES clusters at the M06-2X/6-31++G(d,p) theory level and found that charge transfer from Ch^+ to the HBD in CCU, CCEtg, and CCMal was stronger than the charge transferred between Cl^- and the HBD.[70] Ultimately, Wagle et al. found a correlation between the melting point and the bond order of the $Ch^+\cdots Cl^-$ interaction and not the bond order of the $HBD\cdots Cl^-$ interaction.[70] Yet, when Silva et al. performed a systematic modification of urea in the CCU DES by substituting methyl groups at the amine groups, a combination of Raman spectroscopy and M06-2X calculations found that the melting point depression was governed by the strength of the (urea)N-H$\cdots Cl^-$ interaction.[71] As a final example, Saha et al. optimized a DES cluster of ChCl:acetylsalicylic acid using the ωB97XD theory level.[72] Their CHELPG and natural bond order (NBO) analyses indicated that charge transfer from Cl^- to both Ch^+ and the HBD was the major driving force for the formation of the DES.[72] While the specific details in the literature varied depending on the *ab initio* method utilized and/or the DES investigated, the general argument arising from the gas-phase QM calculations can be summarized as crystallization of the DES mixture at room temperature is hindered through a balance of strong forces present between all components.[73]

However, higher-order QM calculations that include explicit solvation effects have cast doubt upon a simple charge delocalization explanation as the predominant factor in DES melting point depression. For example, charge spreading in CCU, CCGly, and CCOx was investigated by Zahn, Kirchner, and Mollenhauer using *ab initio* molecular dynamics[74] (AIMD), also referred to as first-principles molecular dynamics[75] (FPMD), and a Hirshfeld-I partial charge analysis.[76] They found that hydrogen bonding enhanced negative charge spreading from the anion to the HBD of CCOx and to a lesser extent CCGly. However, in the CCU system, a negligible charge spreading was found as the negative charge of Cl^- was primarily transferred to Ch^+ leaving the urea uncharged. Instead, the urea may behave more as a "spacer" that increases the charge separation of the ions.[77] This suggested that strong disorder in the liquid structure may be more responsible for the low melting points observed in DESs rather than a charge transfer from the anion to the organic compound.[76] Stefanovic et al. corroborated many of these findings in their quantum mechanical molecular dynamics (QM/MD) simulations of CCU, CCEtg, and CCGly nanostructures.[73] Their QM/MD methodology found more subtle structural origins in the melting point depression that include contributions from HBD acidity, HBD structure/conformation, and the extent of HBD self-interaction. For example, strong hydrogen bonding interactions between ChCl and urea was noted for CCU, but more self-interaction by the HBDs in CCEtg, and CCGly led to weaker Cl^- intercalation and a reduced melting point depression.[73] A follow up AIMD study by Zahn examined both the structure and dynamics of CCU.[78] Zahn explored whether the cluster formation, previously predicted by gas-phase QM calculations, was present in the liquid state. Interestingly, the AIMD simulations did not observe the formation of clusters, but instead

found the CCU bulk-phase to resemble molecules rattling in long-living molecular cages.[78, 79] The lack of pairs migrating together suggests that all constituents in CCU have overall similar intermolecular interactions that facilitate a large entropy and supported Zahn's hypothesis of "similia similibus solvuntur" (or "like dissolves like") as the major driving force for melting at room temperature.[78]

3.1.2 Melting point prediction

Less work has been published on the prediction of DES melting points, which may not be surprising given the difficulty in estimating melting points for even simple organic 1:1 salts.[80] García et al. were able to develop a predictive quantitative structure−activity relationship (QSAR) model for ChCl-based DESs by optimizing 29 different HBDS at various molar ratios using B3LYP/6-31+G(d).[81] A seven-parameter QSAR model was developed by selecting the most significant descriptors (from a set of 335 descriptors per HBD) by using a genetic function approximation. The QSAR model gave excellent correlative ability (R^2 = 0.97) and had a high predictive ability (R^2 = 0.93).[81] An alternative and simpler approach was published by Alhadid et al. for preselecting possible DES candidates by qualitatively predicting eutectic temperature based on melting enthalpy.[82]

3.2 Hydrogen bonding

Upon formation of a eutectic mixture, complex hydrogen bonding, e.g., neutral, ionic, and doubly ionic, arises from a network of interactions between neutral molecules and charged species. Accordingly, Stefanovic et al. computed significant hydrogen bond densities of 13.8, 10.8, and 9.4 bonds/nm^3 present for CCU, CCGly, and CCEtg, respectively, which correlated well with their relative viscosities.[73] For a deeper

understanding of these intermolecular interactions, Ashworth et al. performed a systematic and exhaustive DFT-based study to characterize and quantify all potential hydrogen bonding types present in the CCU DES.[77] An “alphabet soup” of 172 hydrogen bonds were identified in contrast to the more homogeneous nature of H-bonds present in molecular solvents. In agreement with Zahn et al.’s AIMD calculations,[76] Ashworth et al. found the cationic urea[Ch]$^+$, i.e., OH···O=C, interaction was the strongest hydrogen bond identified and not urea···Cl$^-$.[77] Instead, the [Cl(urea)$_2$]$^-$ complex was computed to be energetically competitive with both urea[Ch]$^+$ and urea[Cl]$^-$. Hammond et al. supported the computed ordering of hydrogen bond strength proposed by Ashworth et al. through neutron diffraction experiments.[83] Overall, Hammond and Edler best summarized DESs as disordered, entropy-maximized systems featuring hundreds of potential strong and weak hydrogen bonds of different characters and local areas of order.[84] Advancing the current knowledge of hydrogen bonding in heterogeneous DES systems is another area ripe for study using QM methods, such as recent AIMD simulations of DESs with dissolved water[85, 86] and gases, e.g., CO_2 and SO_2.[87, 88]

Vibrational spectroscopy techniques have been applied as a means to characterize the intricate web of hydrogen bonding occurring in DESs and their effect on the melting point, polarity, conductivity, and viscosity.[67, 89-92] For example, Zhu et al. showed that a computational approach using B3LYP-D3 was able to accurately assign vibrational modes measured by Fourier transform infrared spectroscopy (FTIR) and Raman for the CCGly, CCU, and ChCl:acetic acid DESs.[66] In addition, Araujo et al. studied the vibrational modes of CCU using inelastic neutron scattering experiments and discrete and periodic *ab initio* calculations and found that two ChCl and four urea units

are the minimum cluster size needed to computationally represent the most important DES intermolecular interactions (an optimized representation is shown in Figure 3).[93] Interestingly, Araujo et al. also found urea's geometry to be more pyramidal (sp^3) in CCU compared to sp^2 planar in the crystal, which allows for a more flexible hydrogen bond network that encourages eutectic behavior.[93] Finally, Rain et al. computed the IR spectra of nine different ChCl-based DESs using ωB97XD and analyzed the results with principal component analysis (PCA).[94] They found maximum shifts for the -OH functional group of Ch^+ after cluster formation, suggesting active participation in DES formation through hydrogen bonding with the acceptor groups of HBDs.[94]

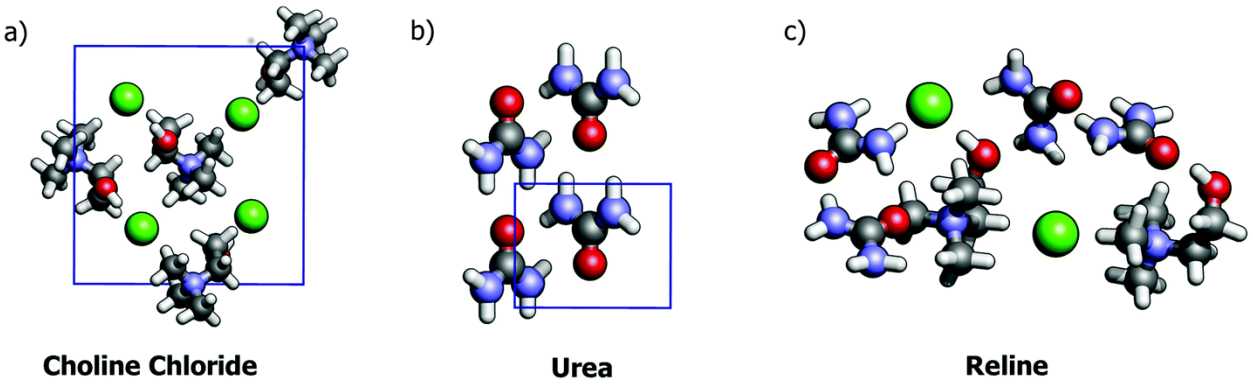

Figure 3. Molecular representation of the crystal lattices of (a) ChCl, (b) urea, and (c) the optimized CCU (or "reline") geometry. Used with permission from C. F. Araujo et al. Inelastic neutron scattering study of reline: shedding light on the hydrogen bonding network of deep eutectic solvents. *Phys.Chem.Chem.Phys.*, **2017**, *19*, 17998-18009. Copyright 2017, The Royal Society of Chemistry.

As the DES field continues to grow, the development of protic DESs may be envisioned as analogous to the protic ionic liquids (PIL) field.[95] As such, future computational studies in protic DES applications, e.g., anhydrous proton-conducting electrolytes in fuel-cell technology, would require a method that could reproduce both

hydrogen bonding and proton diffusion. In this respect, AIMD is the logical method for accurately capturing the Grotthuss mechanism, i.e., proton jumping, in protic solvents.[96] For example, Ingenmey et al. utilized AIMD simulations to approximate the ionicity of a PIL by considering the proton conduction between ionic and neutral species in the system.[97] An additional area where AIMD may excel is for DESs that act as electrolytes containing redox-active species at electrode surfaces.[98]

4. MOLECULAR DYNAMICS

As computational studies expand towards the reproduction of bulk-phase DES thermodynamic and transport properties, the use of QM-based methods quickly become cost prohibitive given the extensive computational resources and time required. As such, classical molecular dynamics (MD) methods are better suited for modeling larger sized DES systems, e.g., hundreds to thousands of ionic/molecular species. However, MD accuracy is dependent upon the availability of suitable force field (FF) parameters. This section highlights efforts to develop and refine DES FF potentials, examines solvent organization alongside thermodynamic and transport properties of DESs, and underscores important conclusions made by *ab initio* methods.

4.1 Force field development

While generalized FFs, such as GAFF[99] and DREIDING,[100] have proven themselves accurate in small molecule and macromolecular systems, the complexity of charged solvents has necessitated in the development and refinement of unique parameter sets, e.g., similar to ionic liquids.[101-103] Force fields provide explicit representation of complex atom-to-atom interactions by incorporating geometric

descriptions of the molecules/ions in the form of bonded interactions, i.e., bonds, angles, and torsions, along with intermolecular forces derived from electrostatic charge distributions and Lennard-Jones terms that account for repulsive and dispersive van der Waals interactions. The reader is referred to an excellent review by Riniker that provides an overview of the classical function form used in major fixed-charge FF families, i.e., AMBER, CHARMM, GROMOS, and OPLS.[104] Tuning these FF parameters towards high-level QM and experimental data was required to improve DES simulation accuracy as described below.

4.1.1 Scaling charges, tuning Lennard-Jones terms, and polarizability

The choice of charge model, e.g., RESP, ChelpG, AIM, and Merz-Kollman, and the method in which the atomic partial charges are derived, i.e., from minimal clusters consisting of a 1:2 salt:HBD ratio or individual molecules/ions, can have a dramatic influence on the predicted structural arrangement of the DES.[105] For example, a systematic study of ten charge sets for CCLev by García, Atilhan, and Aparicio found that the ChelpG[106] and Merz-Kollman[107] charge models in conjunction with the minimal cluster approach yielded the best experimental reproduction of macroscopic properties.[105] Beyond QM-derived partial charges, Doherty and Acevedo tuned empirical charges and adjusted LJ parameters during the development of an OPLS-AA FF for ChCl-based DES systems (called OPLS-DES)[108] to match radial distribution functions (RDFs) derived from liquid-phase neutron diffraction data reported by Hammond, Bowron, and Edler.[83] A potential drawback of this procedure is the transferability of these parameters to simulations featuring complex systems, e.g., additional species or heterogeneous environments.[109] Machine learning methods may offer new opportunities to improve the

accuracy of FFs, as recently shown for partial charges.[110] For example, Zhong, Velez, and Acevedo reported OPLS-AA parameters for DESs constructed from ethylammonium, N,N-diethylethanolammonium, and N-ethyl-N,N-dimethylethanolammonium chloride salts by developing a genetic algorithm approach that automates the creation of partial charges fit to experimental physicochemical properties, e.g., surface tension and viscosity.[111, 112]

Another avenue for improving agreement with experiment is the tuning of nonbonded parameters to treat polarization implicitly. For example, when Ferreira et al. tested various FF combinations for CCEtg using an unscaled charge scheme (±1e), the self-diffusion coefficients of Ch^+ and ethylene glycol were found to be underestimated by a factor of 8 compared to experiment; whereas, they observed large accuracy gains when scaling the atomic partial charges by 0.8.[113] In general, scaling factors between 0.7 and 0.9 have been commonly applied to atomic charges in DES simulations.[105, 108, 114-116] However, scaling charges can have negative consequences, such as reduced FF parameter transferability and an underestimation of the enthalpy and free energy of solvation in mixtures or solutes.[117] Chaumont et al. questioned whether scaling partial charges was even necessary for DESs.[118] Instead, they reported that sole refinement of Lennard-Jones parameters in the GAFF v2.1 FF yielded comparable accuracy in the reproduction of CCEtg and CCGly physicochemical properties.[118] In addition, Kaur et al. successfully utilized unscaled charges with the CHARMM FF to study the solvent organization of bulk CCU[119] and CCEtg.[120] A final alternative to consider is the use of a polarizable FF, as parameters are expected to be more transferable and can remove artificial long-range ordering present in some nonpolarizable FFs for charged solvents;[121]

yet, accuracy gains are balanced with increased computational costs.[122] Jeong, McDaniel, and Yethiraj developed a polarizable FF for CCU by using a symmetry-adapted perturbation theory (SAPT) protocol[123] refit to FPMD simulations and found that including polarizability qualitatively influenced radial distributions, the lifetimes of hydrogen bonds, and affected long-range structural order and dynamics.[124] In addition, Goloviznina et al. expanded their polarizable CL&Pol FF[125] to the simulation of CCEtg with a reasonably accurate structural reproduction of AIMD simulations.[126]

4.2 Solvent organization

The earliest reported MD simulations of DESs came a decade after their initial discovery.[114, 127, 128] Refinement of FF parameters have meant that subsequent classical simulations have continued to improve in the prediction and reproduction of DES physical properties, including density, surface tension, heat capacity, and viscosity.[105, 108, 113, 129-134] Solvent organization can also be easily derived from bulk-phase MD simulations. For example, computed center-of-mass radial distribution functions (RDFs) by Sun et al. revealed that the long-range ordering of intercalating cations and anions in neat ChCl diminished with increasing concentration of urea molecules in CCU.[127] At the typical 1:2 CCU molar ratio, shortened hydrogen bonds and modest interaction energies correlated with the lower melting point.[127] More recently, Celebri et al. utilized Kirkwood–Buff Integrals (KBI)[135] with MD simulations to connect the microstructure of CCU mixtures to thermodynamic and transport properties.[136] They confirmed Sun et al.'s findings that ChCl-ChCl and ChCl-urea interactions become weaker while those between urea-urea become stronger with increasing urea mole fraction.[127, 136] Similarly, Hammond et al.'s study of CCU that coupled liquid-phase neutron diffraction data with an empirical potential

structure refinement model (ND/EPSR) found that urea-urea had the largest average coordination number compared to other constituent interactions (Table 3).[83] Both classical OPLS-DES[108] and QM-based FPMD[85] simulations found substantial coordination between urea-urea and choline-urea (Table 3). However, the dominance of HBD-HBD interactions may be exclusive to CCU, as Perkins, Painter, and Colina found that MD simulations of CCEtg, CCGly, and CCMal favored the HBD-Cl^- interaction instead.[128]

To further investigate the unique role of urea in CCU, Shayestehpour and Zahn performed MD simulations on mixtures of ChCl and urea derivatives[71] and found that the amide hydrogen *trans* to the oxygen of urea maintained a more favorable interaction with Cl^- (-27.3 kJ/mol) compared to the *cis* counterpart (-15.2 kJ/mol), and that both *trans* hydrogens effectively coordinated to a second urea molecule (-21.5 kJ/mol).[137] Migliorati and D'Angelo further examined the anion interactions by simulating analogous Ch^+ and urea DESs that differed only in anionic species, i.e., Cl^-, F^-, NO_3^-, and CH_3COO^-.[138] Their MD simulations found that the order of DES melting points is not related to the strength of urea-anion hydrogen bonds, but instead the ability of the anion to maximize hydrogen bonds between all the different moieties.[138] Finally, Migliorati et al. studied the role of the cation in DESs composed of Cl^- and urea using MD simulations and found that the presence or lack of a hydroxyl group on the cation strongly affected the DES hydrogen bond network with large ramifications on solvent organization.[139]

Table 3. Average Coordination Number (N_{coord}) and Positions (Å) of the First Maximum and Minimum in Center-of-Mass RDFs between Choline Cation (Ch), Chloride Anion (Cl), and Urea in the CCU Deep Eutectic Solvent.

		OPLS-DES (303 K)			ND/ESPR (303 K)[83]			FPMD (333 K)[85]		
center	shell	r_{max}	r_{min}	N_{coord}	r_{max}	r_{min}	N_{coord}	r_{max}	r_{min}	N_{coord}
urea	Cl	4.3	5.4	1.90	4.0	5.5	2.08 ± 1.01	4.1	5.3	1.9 ± 0.4
Ch	Cl	4.1	6.4	3.49	4.2	6.7	4.35 ± 1.30	4.2	6.5	3.1 ± 0.6
Ch	urea	4.7	7.2	8.76	5.4	6.9	5.91 ± 2.84	5.1	7.1	8.6 ± 0.7
Ch	Ch	6.5	8.2	5.41	6.3	8.0	6.74 ± 2.16	-	-	-
urea	urea	4.8	6.6	6.00	4.3	6.1	6.77 ± 3.05	4.7	6.3	4.9 ± 0.5

4.3 Thermodynamic and transport properties

4.3.1 Heats of vaporization

Calculating the heat of vaporization (ΔH_{vap}) for a DES can be tricky as the vapor phase composition is experimentally unknown. In a systematic study of DES vaporization, Salehi et al. performed MD simulations with three unique clusters escaping into the gas phase, i.e., HBD, HBA, and HBA:HBD.[140] They postulated that the component least "bound" to the system would most likely dominate the vapor phase. Accordingly, the ΔH_{vap} computed for CCU, CCEtg, CCGly, CCMal, and CCOx using OPLS-AA parameters by Doherty and Acevedo[108] found that sole vaporization of the more volatile HBDs yielded closer agreement with experiment.[140] For example, ΔH_{vap} values for CCU derived from the vaporization of urea, ChCl, and a ChCl-urea cluster were 82, 165, and 228 kJ/mol, respectively, compared to experimental estimates of 46.9 and 79.0 kJ/mol[140] derived from

fitting vapor pressure data reported by Shahbaz et al.[141] and Ravula et al.[142] The alternative use of GAFF parameters for CCU from Perkins et al.[128] gave reduced accuracy when computing ΔH_{vap} but concurred with OPLS-AA that the HBD should dominate the vapor phase composition.[140] In other work, Ferreira et al. tested various combinations of mixed FF parameters for CCEtg to compute ΔH_{vap} from the vaporization of ethylene glycol, ChCl, and a ChCl-ethylene glycol cluster and found large ranges of 133.7–324, 232.5–307.9, and 167.5–179.5 kJ/mol for each species, respectively.[113] Their computed ΔH_{vap} values were overestimated when compared to the experimental approximation of 55.8 kJ/mol[140] or 73 kJ/mol when computed with OPLS-AA.[108, 140] Ferreira et al followed a similar procedure to calculate ΔH_{vap} values for CCPro in separate work.[143] In general, while experimentally measured vapor pressures of DESs are quite close to the vapor pressures of their respective pure HBDs,[140] MD simulations have provided evidence that some proportion of the HBA components should be present in the gas phase of DESs.[144]

4.3.2 Self-diffusion coefficients

Diffusion coefficients studies by D'Agostino et al.[67] and Abbott et al.[89] featuring pulse field gradient nuclear magnetic resonance (PFG)-NMR have indicated that diffusivity in DESs is dictated by a combination of hole theory[145] and the strength of the hydrogen bonding network present in the solvent. In modified hole theory,[146] ions diffuse by moving between vacancies when an ion's hole size is smaller than an adjacent hole (Figure 4). Accordingly, D'Agostino et al. found a very good correlation between diffusion rate and the amount of free volume available for the species in the DES compound.[67] This suggests that diffusion in DESs may proceed via a hopping mechanism similar to

ionic liquids.[67] Hole theory also explains why cations diffuse slower than HBDs, such as urea, glycerol, and ethylene glycol; however, malonic acid in CCMal is an exception given its ability to dimerize through hydrogen bonding of the carboxylic acid functional groups.[67] In terms of the influence of the DES hydrogen bond network in diffusivity, Abbott et al. showed that increasing the concentration of ChCl in CCGly beyond the usual 1:2 molar ratio breaks intermolecular forces present between the glycerol molecules leading to enhanced mobility for each component.[89]

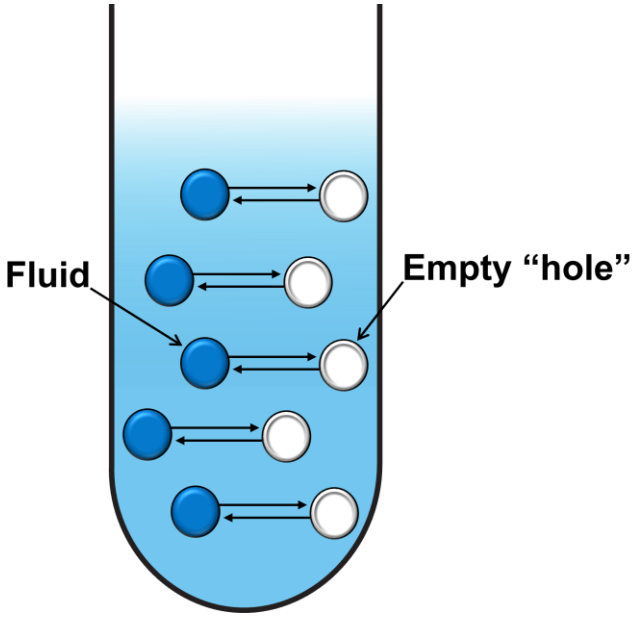

Figure 4. Hole theory for liquids assumes the solvent continuum is permeated by holes that explain transport, thermal, and viscous properties in liquids at equilibrium. Adapted with permission from C. D’Agostino Hole theory as a prediction tool for Brownian diffusive motion in binary mixtures of liquids. *RSC Adv.*, **2017**, *7*, 51864-51869. Copyright 2017, The Royal Society of Chemistry.

Self-diffusion coefficients are typically computed by applying the Einstein relation and the average mean square displacement for each constituent's center of mass.[147] It is important that the simulated system is within a proper diffusive regime where ions/molecules are moving freely, which is typically monitored through the calculation of a beta-parameter (β).[148] As discussed earlier, employing integer charges (±1 e) when using nonpolarizable FFs has been shown to significantly underestimate the diffusion coefficients, e.g., Mainberger et al. reported 92% errors in the self-diffusion coefficients of CCGly when using unscaled MMFF parameters.[116] Scaling charges can provide considerable improvement. For example, Ferreira et al. reported MD simulations using unscaled Perkins et al. charges[114] for CCEtg that gave errors of 90.13% and 87.88% for Ch^+ and ethylene glycol, respectively; the errors were dramatically improved to 11.8% and 2.8% when scaling the same charges by 0.8.[113] Ferreira et al. also tested a system specific 0.74 charge scaling for CCPro and found larger errors of 17% and 15% for Ch^+ and propylene glycol self-diffusion coefficients, respectively.[113]

An additional consideration when computing self-diffusion coefficients is the temperature of the simulation. Perkins et al. showed that self-diffusion coefficient errors in CCU, CCEtg, and CCGly were considerably improved at higher temperatures, e.g., 51.4% and 40.9% for Ch^+ and urea in CCU at 298 K compared to 3.8% and 3.4% at 330 K.[114, 128] However, even at 330 K, errors as large as 27% were reported for other DES systems.[102, 114] Doherty and Acevedo also found considerable improvement for 8 unique DESs when using empirical charges scaled by 0.8 and simulation temperatures of 400.15-500.15 K with the calculated diffusion coefficient extrapolated to room temperature.[108] However, the agreement varied substantially, e.g., in the CCU system

errors were reported as 31.4%, 0.0%, and 23.2% for 298.15 K, 308.15K, and 323.15 K, respectively.[108] Although calculated self-diffusion coefficients can appear accurate at specific temperatures, there exists an inconsistency in nonpolarizable FFs when tested over a range of temperatures that yield a parabola-like temperature dependence with percent errors more than doubled between temperatures.[108, 113] To further emphasize the challenge of accurately calculating self-diffusivity in DES, we refer once again to the polarizable FF for CCU by Jeong et al. that yielded a substantial factor of 3 error when compared to experiment.[124] In addition, the polarizable CL&Pol FF greatly overestimated the diffusion coefficient for the HBD in the simulation of CCEtg.[126] Further reparameterization of polarizable FFs to improve agreement presents a major challenge as the slow dynamics of DESs necessitates in impractically long time lengths to achieve statistically accurate results.[124] New methods or approaches, perhaps encompassing machine learning or FFs with explicit inclusion of charge transfer,[149, 150] will be required to achieve accurate self-diffusivity reproduction and prediction for DESs. As one considers the potential for dramatic computational advances over the next 25 years, it is not difficult to imagine a day when FFs could be completely replaced with low-cost QM methods, particularly for solvent systems such as DESs.[151]

5. MACHINE LEARNING

5.1 A primer on machine learning

Artificial intelligence (AI) in machines can be succinctly defined as reusing the feedback from prior calculations to continuously improve predictions without manual modification of the code.[152] Machine learning (ML) in turn is a sub-field of AI that utilizes

statistical methods to solve specific tasks, which in the context of chemistry can guide scientific discovery in the space of limitless molecules and synthetic pathways.[153-156] ML regression algorithms (or classifiers), such as Generalized linear models (GLM), Neural networks (NN), and Support vector machines (SVM),[157] correlate large data sets to yield desired chemical predictions by using artificial features that do not necessarily correspond to the physical properties of the molecular system. NNs mimic a biological approach that places positive and negative weights between nodes to indicate excitatory and inhibitory connections, respectively. Whereas SVM depicts training data as vectors in space with the widest possible gap and tries to categorize new data into the appropriate side of the gap.[158] Ultimately, transforming raw data into more abstract forms better suited to fit complex equations led to the development of Deep Learning (DL), a sub-field of ML that excels at discovering intricate structures in high-dimensional data.[159] It is important to note that most regression models create a curve with the minimum possible residual distance from the measured points and not through all available data points. Consequently, overfitting of the data can occur in the space of limited data or in an overly complex model featuring many parameters.[160, 161] In addition, a ML algorithm that cannot properly capture the underlying structure of the data, i.e., underfitting, will also lead to poor predictions.

Artificial neural networks (ANNs), a sub-field of DL, are composed of multiple node layers, containing an input layer, one or more hidden layers, and an output layer (Figure 5). Each node is connected to another with an associated weight and a threshold that determines if the node is activated. In a typical ANN system, there may be hundreds of millions of these adjustable weights, and millions of examples to train the algorithm.

These successive layers of processing units correlate the artificial features from the raw data to yield the property prediction in the final layer. An ANN possessing more than three hidden layers is characteristically defined as a deep neural network (DNN) (Figure 5). ANNs are arguably the most widely applied AI method in chemical research and, most relevant to this review, in the related field of ionic liquids; Koutsoukos et al. have written an excellent review highlighting the use of multiple ML methods for the IL chemical space.[162] In their publication, the authors pointed out that while the IL field is heavily computer-aided (with thousands of published papers featuring MD, QM, Monte Carlo, etc.), the use of ML in IL research is extremely limited with ~30 papers published per year between 2018 and 2020. In many ways this echoes what is occurring in the DES field (which of course are IL analogues) as the reported use of ML for DES property prediction is extremely limited.

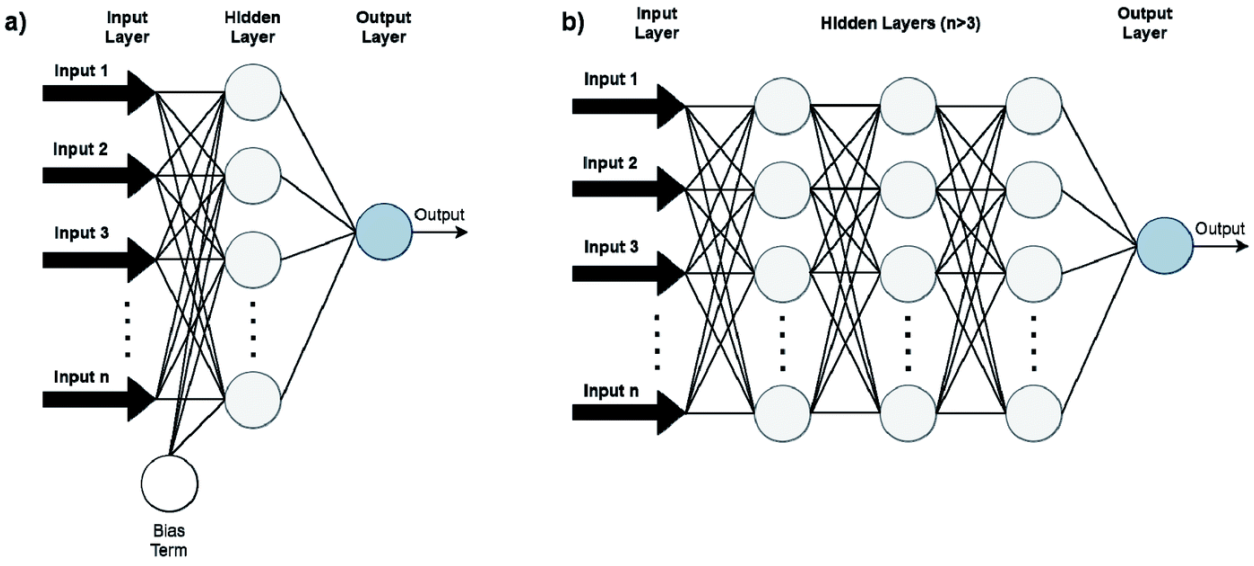

Figure 5. Conventional feed-forward artificial neural networks (ANNs) (a) differ from deep neural networks (DNNs) (b) by having only one hidden neuron layer. Bias terms (output of the NNs when input is zero) are not connected in DNN for simplicity. Used with permission from S. Koutsoukos, F. Philippi, F. Malaret, T. Welton, *Chem. Sci.*, **2021**, *12*,

6820-6843**.** A Review on Machine Learning Algorithms for the Ionic Liquid Chemical Space. Copyright 2021, The Royal Chemical Society.

5.2 Physical properties from artificial neural networks

5.2.1 Density

The density of a DES is an important physical property for solvent characterization; however, experimental evaluation of densities may not always be practical, e.g., as a function of temperature. Estimation methods for DES density predictions have been reported,[163] but the use of ANNs could provide more accurate results. Accordingly, Shahbaz et al. developed and trained an ANN using measured densities over a temperature range of 298.15 to 368.15 K for three classes of DESs based on the salts of methyltriphenylphosphonium bromide, N,N-diethylethanolammonium chloride, and ChCl.[164] These DESs featured glycerol and ethylene glycol as the HBDs in different molar ratios. Shahbaz et al. applied a three-layer back propagation neural network with 9 neurons in the hidden layer. A dataset of 270 densities across a range of temperatures and compositions were divided randomly into training and evaluation (60%) and simulation (40%). A comparison between the ANN-predicted densities and those obtained by measurement yielded an absolute relative percentage error (ARPE) of 0.14%, which was considerably improved over the authors' previous group contribution method[163] which gave an ARPE of 2.03% for the same set of DESs.[164]

Adeyemi et al. also trained an ANN to predict the densities of DESs composed of ChCl and the HBDs of monoethanolamine, diethanolamine, and methyldiethanolamine in molar ratios of 1:6, 1:8, and 1:10 at temperatures of 293.15–353.15 K.[165] A feed-forward three-layer back propagation conventional ANN with 10 neurons in the hidden layer was

trained using 55% of the 105 total experimental data points. In addition, a bagging ANN was developed by the authors where a collection (ensemble) of conventional ANNs were selected, trained with resampling from bootstrap, and their predictions combined. The neural networks gave average absolute relative deviations (AARD) in the range of 0.17-1.35% when using the conventional ANN and 0.01-0.08% for the bagging ANN compared to experimental densities. Densities were also predicted using an empirical group contribution method (i.e., the modified Rackett equation),[166] but gave a significantly worse error range of 5.81-7.03%.

5.2.2 Electrical conductivity

Electrical conductivity is a fundamental physical property that describes the degree to which a material conducts electricity (and is the reciprocal of resistivity). Accurate predictions of conductivity are crucial for the adoption of prospective DESs into industrial electrochemical processes, e.g., corrosion prevention.[167] Correspondingly, Ghareh Bagh et al. created and trained an ANN using experimental measurements of electrical conductivity for DESs composed of ChCl, N,N-diethylethanolammonium chloride, and methyltriphenylphosphonium bromide as the source of salts with varying mole fractions of glycerol and ethylene glycol as the HBDs.[168] Temperatures between the range of 298.15 and 353.15 K in 5 K intervals were used at 1 atm. A feed-forward three-layer back propagation neural network was utilized to predict electrical conductivity. The optimal ANN architecture was determined to contain 8 neurons within a single hidden layer after testing a range of 1-30 neurons. 216 experimental data points were used with 50% of the data reversed for training, 25% for validation, and the remainder for testing the accuracy of the ANN electrical conductivity predictions. An AARD value of 4.40% was computed

compared to experiment and a regression coefficient (R^2) value of 0.9983 was reported.[168]

Electrical conductivity prediction for DESs was also investigated by Adeyemi et al. during their development of the conventional and bagging ANNs as discussed previously in their DES density predictions.[165] Their ANN models of alkanolamine-ChCl DESs aimed to improve the accuracy achieved by the ANN 6-8-1 architecture reported by Ghareh Bagh et al. for ammonium and phosphonium based DESs.[168] A statistical assessment of their conventional and bagging ANNs yielded a normalized mean square error (NMSE) of 5.9384×10^{-2} and 5.82×10^{-4}, respectively, when compared to experimental conductivity measurements. Overall, a major improvement in accuracy was found for the bagging ANN method over the conventional ANN for both conductivity and density.[165]

5.2.3 Viscosity

High viscosity is characteristically observed in DESs and is a major drawback in many industrial processes, e.g., impeding flow and decreasing the mass transfer rate of solutes in solvent extractions. While the addition of co-solvents, changing salt:HBD molar ratios, or the use of elevated temperature can help reduce viscosity,[169-171] the ability to computationally predict and create less viscous DESs would be ideal. However, the nonideality of the solvent mixtures and hydrogen bonding present in the system makes DES viscosity prediction challenging.[46] In the work of Benguerba et al. a predictive viscosity model was created using a combination of multilinear regression (MLR) and ANN methods.[172] In their work, a literature-based data set of 108 experimental viscosity measurements was assembled from DESs composed of methyltriphenylphosphonium

bromide, ChCl, and tetrabutylammonium bromide and the HBDs monoethanolamine, diethanolamine, and methyldiethanolamine. Benguerba et al. used a quantitative structure property relationships (QSPR) approach[173, 174] where computed $S_{\sigma\text{-profile}}$ and temperature MLR model descriptors were used in the framework of an ANN model featuring a three-layer feed-forward neural network with 3 hidden neurons.[172] The ANN was trained on 72 data points with the remaining 36 data points used for validation. The values of statistical indicators for the ANN model (R^2 = 0.9863 and RMSE = 0.1288) indicated good agreement with experimental measurements and a significant improvement over the simple MLR model (R^2 = 0.9305).[172] As a word of caution, it should be noted that the highly viscous nature of DESs often leads to major inconsistencies in the literature under identical conditions. For example, viscosities for CCU at ambient conditions have been reported to range from 152 cP[16] to 527.28 cP.[170] Hence, great care is required when assembling a DES viscosity database for ML training.

5.2.4 Future Directions in Machine Learning for DESs

While the present focus of ML in DESs studies has been on property prediction from large databases, one can imagine future efforts that are built upon the developmental ANN work of Behler and Parrinello[175, 176] or the Gaussian Approximation Potential (GAP) by Csányi[177, 178] for chemical systems. These ML methodologies could be implemented into existing modeling frameworks that substitute DFT or higher-level QM computed potential-energy surfaces with a neural-network representation.[179] Previously discussed limitations of classical MD simulations, e.g., self-diffusivity errors, could be improved by utilizing energies or forces derived from ANNs trained on AIMD trajectories. However, bypassing expensive electronic structure calculations to access

long time scales and model larger systems will require a significant amount of QM data for ML training that may be extremely difficult to produce. For example, the creation of such a database may require millions of *ab initio* calculations on individual DES clusters, i.e., similar to the calculated data set of 20 million off-equilibrium conformations for organic molecules reported by Smith et al. in the development of the ANI-1 neural network.[180] Despite all the conceptual, theoretical, and practical challenges needed to be solved in order to incorporate ML into computational simulations,[181] the promise of dramatic breakthroughs in the modeling of DES-based properties and materials provides significant motivation for continued innovation.

6. CONCLUSIONS

Deep eutectic solvents are an exciting class of solvent that have received a considerable amount of attention over the past two decades given the numerous reported advantages that include low cost, a facile synthesis and purification process, and a 100% atom utilization rate. DESs have been categorized into five major classes, i.e., *Types I-V* based on the complexing agent present, with an overwhelming majority of published research focused on the *Type III* class. These DESs are composed from a eutectic composition of HBAs (such as quaternary ammonium halide salts) and molecular HBDs that possess significant melting point depressions, e.g., 12 °C for CCU, relative to their isolated components, i.e., 302 and 133 °C for ChCl and urea. With an estimated 10^6−10^8 possible binary combinations, the construction of novel DESs tailored towards specific applications can quickly become intractable when using an uneducated trial-and-error approach that may easily override any potential advantages provided by the solvent. Fortunately, multiple experimental and computational investigations have enhanced our

fundamental understanding of the complex solvent structure and the unique electrostatic interactions present between the constituents. Despite the immense progress, even basic concepts, such as the origin of the DES melting point depression, are still under debate. As such, fast computational tools capable of making accurate predictions of DES physiochemical properties exclusively from molecular structure would represent a paradigm shift in the field.

Theoretical investigations of DESs have relied heavily on QM modeling to help elucidate their physical, thermodynamic, and structural relationships. The properties of DESs are controlled primarily by interaction energies present between the different components of the mixture. QM calculations performed on small gas-phase structures and clusters have helped to characterize and quantify the “alphabet soup” of hundreds of potential hydrogen bonds present in DESs. Reproduction of vibrational spectroscopy measurements and examination of charge transfer between the constituents have aided in elucidating the source of the characteristic DES melting point depression. However, the exclusion of explicit solvation effects has led to some inconsistencies that were brought to light by higher-order QM methods. For example, AIMD (or FPMD) simulations have shown that the predominant factor in DES melting point depression may not be the simple charge delocalization proposed by the gas-phase QM calculations. Instead, more subtle structural origins in the melting point depression may be at play that include contributions from HBD acidity, HBD structure/conformation, and the extent of HBD self-interaction. Alas, further investigation into the thermodynamic and transport properties of DESs using AIMD becomes near impossible given the severe limitations in trajectory lengths and smaller system sizes imposed by the large computational resources required.

Classical MD methods are better suited for modeling DES systems featuring thousands of ionic/molecular species. However, the complexity of the charged solvents has necessitated in extensive development and validation of new FF parameters. In general, most published ChCl-based nonpolarizable FFs accurately reproduce many experimental bulk-phase DES physiochemical properties, e.g., density, thermal expansion coefficient, surface tension, heat capacity, viscosity, and solvent organization. Major gains in accuracy were reported when scaling atomic charges and tuning Lennard-Jones terms towards neutron diffraction data and AIMD simulations of pure DESs. However, modeling more complex DES systems that feature additional species or heterogeneous environments have resulted in larger errors suggesting that alternative FF functional forms or the use of a polarizable FF may be required in such cases. Nevertheless, MD simulations have provided great insight into solvent organization for multiple DESs and have examined the subtleties of vapor phase composition in heats of vaporization measurements. A major challenge for nonpolarizable FFs has been the poor reproduction of self-diffusion coefficients; unfortunately, explicit treatment of polarization has not significantly improved predictions. New methods, perhaps encompassing machine learning, may be required to achieve accurate self-diffusivity replication. While the ML field is currently experiencing exponential growth, its use in DES research has been extremely limited. Recent ML applications in DES studies include the use of genetic algorithms to improve the accuracy of FF parameters and employing neural networks to make predictions of density, electrical conductivity, and viscosity. In the future, the incorporation of ML methodology into existing modeling frameworks could potentially yield

new and highly accurate methods, e.g., classical MD simulations that utilize energies or forces derived from neural networks trained on AIMD data.

In conclusion, the development and application of simulation methods to DESs over the past decade has led to tremendous advances in our fundamental understanding of these unique systems. However, given their complexity and large potential, many more computational efforts will be needed, particularly beyond the heavily studied *Type III* combinations.

ACKNOWLEDGEMENTS

Gratitude is expressed to the National Science Foundation (CHE-2102038) for support of this research.

CONFLICT OF INTEREST

The authors have declared no conflicts of interest for this article.

DATA AVAILABILITY STATEMENT

Data sharing is not applicable to this article as no new data was created or analyzed in this study.

AUTHOR CONTRIBUTIONS

Caroline Velez: Writing-original draft (equal). **Orlando Acevedo:** Conceptualization (lead); supervision (lead); funding acquisition (lead); writing-original draft (equal).

ORCID

Orlando Acevedo, https://orcid.org/0000-0002-6110-3930

7. REFERENCES

1. Lipshutz BH, Gallou F, Handa S. Evolution of Solvents in Organic Chemistry. ACS Sustain Chem Eng. 2016;4:5838–49.
2. Jordan A, Stoy P, Sneddon HF. Chlorinated Solvents: Their Advantages, Disadvantages, and Alternatives in Organic and Medicinal Chemistry. Chem Rev. 2021;121:1582-622.
3. Clarke CJ, Tu W-C, Levers O, Bröhl A, Hallett JP. Green and Sustainable Solvents in Chemical Processes. Chem Rev. 2018;118:747-800.
4. Byrne FP, Jin S, Paggiola G, Petchey THM, Clark JH, Farmer TJ, et al. Tools and techniques for solvent selection: green solvent selection guides. Sustain Chem Process. 2016;4:7.
5. Welton T. Solvents and sustainable chemistry. Proc R Soc A. 2015;471:20150502.
6. Bubalo MC, Vidović S, Redovniković IR, Jokić S. Green solvents for green technologies. J Chem Technol Biotechnol. 2015;90:1631-9.
7. Pollet P, Davey EA, Ureña-Benavides EE, Eckert CA, Liotta CL. Solvents for sustainable chemical processes. Green Chem. 2014;16:1034-55.
8. Horváth IT, Anastas PT. Innovations and Green Chemistry. Chem Rev. 2007;107:2169–73.
9. Achkar TE, Greige-Gerges H, Fourmentin S. Basics and properties of deep eutectic solvents: a review. Environ Chem Lett. 2021;19:3397–408.
10. Hansen BB, Spittle S, Chen B, Poe D, Zhang Y, Klein JM, et al. Deep Eutectic Solvents: A Review of Fundamentals and Applications. Chem Rev. 2021;121:1232–85.
11. Kaur S, Kumari M, Kashyap HK. Microstructure of Deep Eutectic Solvents: Current Understanding and Challenges. J Phys Chem B. 2020;124:10601–16.
12. Smith EL, Abbott AP, Ryder KS. Deep Eutectic Solvents (DESs) and Their Applications. Chem Rev. 2014;114:11060–82.
13. A. Paiva RC, Aroso I, Martins M, Reis RL, Duarte ARC. Natural Deep Eutectic Solvents – Solvents for the 21st Century. ACS Sustain Chem Eng. 2014;2:1063-71.
14. Tang B, Row KH. Recent developments in deep eutectic solvents in chemical sciences. Monatsh Chem. 2013;144:1427–54.
15. Yu D, Xue Z, Mu T. Eutectics: formation, properties, and applications. Chem Soc Rev. 2021;50:8596-638.
16. Abbott AP, Capper G, Davies DL, Rasheed RK, Tambyrajah V. Novel solvent properties of choline chloride/urea mixtures. Chem Commun. 2003:70-1.
17. Ruß C, König B. Low melting mixtures in organic synthesis – an alternative to ionic liquids? Green Chem. 2012;14:2969-82.
18. Zhang Q, Vigier KDO, Royer S, Jerome F. Deep eutectic solvents: syntheses, properties and applications. Chem Soc Rev. 2012;41:7108-46.
19. Sheldon RA, Woodley JM. Role of Biocatalysis in Sustainable Chemistry. Chem Rev. 2018;118:801-38.
20. Mbous YP, Hayyan M, Hayyan A, Wong WF, Hashim MA, Looi CY. Applications of deep eutectic solvents in biotechnology and bioengineering-Promises and challenges. Biotechnol Adv. 2017;35:105-34.

21. Maia RA, Louis B, Baudron SA. Deep eutectic solvents for the preparation and post-synthetic modification of metal- and covalent organic frameworks. CrystEngComm. 2021;23:5016-32.
22. Tomé LC, Mecerreyes D. Emerging Ionic Soft Materials Based on Deep Eutectic Solvents. J Phys Chem B. 2020;124:8465-78.
23. Wagle DV, Zhao H, Baker GA. Deep Eutectic Solvents: Sustainable Media for Nanoscale and Functional Materials. Acc Chem Res. 2014;47:2299–308.
24. Nahar Y, Thickett SC. Greener, Faster, Stronger: The Benefits of Deep Eutectic Solvents in Polymer and Materials Science. Polymers (Basel). 2021;13:447.
25. Jablonský M, Škulcová A, Šima J. Use of Deep Eutectic Solvents in Polymer Chemistry-A Review. Molecules. 2019;24:3978.
26. Roda A, Matias AA, Paiva A, Duarte ARC. Polymer Science and Engineering Using Deep Eutectic Solvents. Polymers (Basel). 2019;11:912.
27. Carriazo D, Serrano MC, Gutiérrez MC, Ferrer ML, del Monte F. Deep-eutectic solvents playing multiple roles in the synthesis of polymers and related materials. Chem Soc Rev. 2012;41:4996-5014.
28. Redha AA. Review on Extraction of Phenolic Compounds from Natural Sources Using Green Deep Eutectic Solvents. J Agric Food Chem. 2021;69:878–912.
29. Huang J, Guo X, Xu T, Fan L, Zhou X, Wu S. Ionic deep eutectic solvents for the extraction and separation of natural products. J Chromatogr A. 2019;1598:1-19.
30. Li X, Row KH. Development of deep eutectic solvents applied in extraction and separation. J Sep Sci. 2016;39:3505-20.
31. Ruesgas-Ramón M, Figueroa-Espinoza MC, Durand E. Application of Deep Eutectic Solvents (DES) for Phenolic Compounds Extraction: Overview, Challenges, and Opportunities. J Agric Food Chem. 2017;65:3591-601.
32. Olives AI, González-Ruiz V, Martín MA. Sustainable and Eco-Friendly Alternatives for Liquid Chromatographic Analysis. ACS Sustain Chem Eng. 2017;5:5618–34.
33. Li X, Binnemans K. Oxidative Dissolution of Metals in Organic Solvents. Chem Rev. 2021;121:4506–30.
34. Farrán A, Cai C, Sandoval M, Xu Y, Liu J, Hernáiz MJ, et al. Green Solvents in Carbohydrate Chemistry: From Raw Materials to Fine Chemicals. Chem Rev. 2015;115:6811-53.
35. Pelaquim FP, Neto AMB, Dalmolin IAL, Costa MCd. Gas Solubility Using Deep Eutectic Solvents: Review and Analysis. Ind Eng Chem. 2021;60:8607-20.
36. Chen Y, Han X, Liu Z, Yu D, Guo W, Mu T. Capture of Toxic Gases by Deep Eutectic Solvents. ACS Sustainable Chem Eng. 2020;8:5410–30.
37. Atilhan M, Aparicio S. Review and Perspectives for Effective Solutions to Grand Challenges of Energy and Fuels Technologies via Novel Deep Eutectic Solvents. Energy Fuels. 2021;35:6402–19.
38. Troter DZ, Todorović ZB, Đokić-Stojanović DR, Stamenković OS, Veljković VB. Application of Ionic Liquids and Deep Eutectic Solvents in Biodiesel Production: A Review. Renew Sustain Energy Rev. 2016;61:473-500.
39. Gertrudes A, Craveiro R, Eltayari Z, Reis RL, Paiva A, Duarte ARC. How Do Animals Survive Extreme Temperature Amplitudes? The Role of Natural Deep Eutectic Solvents. ACS Sustainable Chem Eng. 2017;5:9542–53.

40. Kim KH, Eudes A, Jeong K, Yoo CG, Kim CS, Ragauskas A. Integration of renewable deep eutectic solvents with engineered biomass to achieve a closed-loop biorefinery. Proc Natl Acad Sci USA. 2019;116:138216-13824.
41. Soh L, Eckelman MJ. Green Solvents in Biomass Processing. ACS Sustain Chem Eng. 2016;4:5821–37.
42. Wazeer I, Hayyan M, Hadj-Kali MK. Deep eutectic solvents: designer fluids for chemical processes. J Chem Technol Biotechnol. 2018;93:945-58.
43. Alonso DA, Baeza A, Chinchilla R, Guillena G, Pastor IM, Ramón DJ. Deep Eutectic Solvents: The Organic Reaction Medium of the Century. Eur J Org Chem. 2016;2016:612-32.
44. Liu P, Hao J-W, Mo L-P, Zhang Z-H. Recent advances in the application of deep eutectic solvents as sustainable media as well as catalysts in organic reactions. RSC Adv. 2015;5:48675-704.
45. Beyersdorff T, Schubert TJS, Welz-Biermann U, Pitner W, Abbott AP, McKenzie KJ, et al. Electrodeposition From Ionic Liquids. MacFarlane DR, Abbott AP, editors: Wiley-VCH: Weinheim; 2008.
46. Alkhatib III, Bahamon D, Llovell F, Abu-Zahra MRM, Vega LF. Perspectives and guidelines on thermodynamic modelling of deep eutectic solvents. J Mol Liq. 2020;298:112183.
47. Wagle DV, Adhikari L, Baker GA. Computational perspectives on structure, dynamics, gas sorption, andbio-interactions in deep eutectic solvents. Fluid Ph Equilibria. 2017;448:50-8.
48. Wilkes JS, Levisky JA, Wilson RA, Hussey CL. Dialkylimidazolium chloroaluminate melts: a new class of room-temperature ionic liquids for electrochemistry, spectroscopy and synthesis. Inorg Chem. 1982;21:1263-4.
49. Abbott AP, Capper G, Davies DL, Munro HL, Rasheed RK, Tambyrajah V. Preparation of Novel, Moisture-Stable, Lewis-Acidic Ionic Liquids Containing Quaternary Ammonium Salts with Functional Side Chains. Chem Commun. 2001:2010-1.
50. Abbott AP, Boothby D, Capper G, Davies DL, Rasheed RK. Deep eutectic solvents formed between choline chloride and carboxylic acids: versatile alternatives to ionic liquids. J Am Chem Soc. 2004;126:9142-7.
51. Lei Z, Chen B, Koo Y-M, MacFarlane DR. Introduction: Ionic Liquids. Chem Rev. 2017;117:6633–5.
52. Welton T. Room-Temperature Ionic Liquids. Solvents for Synthesis and Catalysis. Chem Rev. 1999;99:2071-84.
53. Hallett JP, Welton T. Room-Temperature Ionic Liquids: Solvents for Synthesis and Catalysis. 2. Chem Rev. 2011;111:3508-76.
54. Khandelwal S, Tailor YK, Kumar M. Deep eutectic solvents (DESs) as eco-friendly and sustainable solvent/catalyst systems in organic transformations. J Mol Liq. 2016;215:345-86.
55. Radošević K, Bubalo MC, Srček VG, Grgas D, Dragičević TL, Redovniković IR. Evaluation of toxicity and biodegradability of choline chloride based deep eutectic solvents. Ecotoxicol Environ Saf. 2015;112:46-53.
56. Abbott AP, Barron JC, Ryder KS, Wilson D. Eutectic-Based Ionic Liquids with Metal-Containing Anions and Cations. Chem Eur J. 2007;13:6495 – 501.

57. Abbott AP, Capper G, Davies DL, Rasheed RK. Ionic Liquid Analogues Formed from Hydrated Metal Salts. Chem Eur J. 2004;10:3769-74.
58. Abranches DO, Martins MAR, Silva LP, Schaeffer N, Pinho SP, Coutinho JAP. Phenolic hydrogen bond donors in the formation of non-ionic deep eutectic solvents: the quest for type V DES. Chem Commun. 2019;55:10253-6.
59. Schaeffer N, Abranches DO, Silva LP, Martins MAR, Carvalho PJ, Russina O, et al. Non-Ideality in Thymol + Menthol Type V Deep Eutectic Solvents. ACS Sustainable Chem Eng. 2021;9:2203–11.
60. Cao J, Su E. Hydrophobic deep eutectic solvents: the new generation of green solvents for diversified and colorful applications in green chemistry. J Clean Prod. 2021;314:127965.
61. Osch DJGPv, Dietz CHJT, Warrag SEE, Kroon MC. The Curious Case of Hydrophobic Deep Eutectic Solvents: A Story on the Discovery, Design, and Applications. ACS Sustain Chem Eng. 2020;8:10591-612.
62. Gurkan B, Squire H, Pentzer E. Metal-Free Deep Eutectic Solvents: Preparation, Physical Properties, and Significance. J Phys Chem Lett. 2019;10:7956-64.
63. Liu Y, Friesen JB, McAlpine JB, Lankin DC, Chen S-N, Pauli GF. Natural Deep Eutectic Solvents: Properties, Applications, and Perspectives. J Nat Prod. 2018;81:679-90.
64. Haghbakhsh R, Raeissi S, Duarte ARC. Group contribution and atomic contribution models for the prediction of various physical properties of deep eutectic solvents. Sci Rep. 2021;11:6684.
65. Kovács A, Neyts EC, Cornet I, Wijnants M, Billen P. Modeling the Physicochemical Properties of Natural Deep Eutectic Solvents. ChemSusChem. 2020;13:3789-804.
66. Zhu S, Li H, Zhu W, Jiang W, Wang C, Wu P, et al. Vibrational analysis and formation mechanism of typical deep eutectic solvents: An experimental and theoretical study. J Mol Graph Model. 2016;68:158-75.
67. D'Agostino C, Harris RC, Abbott AP, Gladden LF, Mantle MD. Molecular motion and ion diffusion in choline chloride based deep eutectic solvents studied by 1H pulsed field gradient NMR spectroscopy. Phys Chem Chem Phys. 2011;13:21383-91.
68. Bader RFW. Atoms in Molecules: A Quantum Theory. Oxford: Oxford University Press; 1994.
69. García G, Atilhan M, Aparicio S. An approach for the rationalization of melting temperature for deep eutectic solvents from DFT. Chem Phys Lett. 2015;634:151-5.
70. Wagle DV, Deakyne CA, Baker GA. Quantum Chemical Insight into the Interactions and Thermodynamics Present in Choline Chloride Based Deep Eutectic Solvents. J Phys Chem B. 2016;120:6739-46.
71. Silva LP, Araujo CF, Abranches DO, Melle-Franco M, Martins MAR, Nolasco MM, et al. What a difference a methyl group makes - probing choline-urea molecular interactions through urea structure modification. Phys Chem Chem Phys. 2019;21:18278-89.
72. Saha M, Rahman MS, Hossain MN, Raynie DE, Halim MA. Molecular and Spectroscopic Insights of a Choline Chloride Based Therapeutic Deep Eutectic Solvent. J Phys Chem A. 2020;124:4690-9.
73. Stefanovic R, Ludwig M, Webber GB, Atkin R, Page AJ. Nanostructure, hydrogen bonding and rheology in choline chloride deep eutectic solvents as a function of the hydrogen bond donor. Phys Chem Chem Phys. 2017;19:3297-306.

74. Tuckerman ME. Ab initio molecular dynamics: basic concepts, current trends and novel applications. J Phys: Condens Matter. 2002;14:R1297.
75. Rimsza JM, Corrales LR. Adsorption complexes of copper and copper oxide in the deep eutectic solvent2:1 urea–choline chloride. Comput Theor Chem. 2012;987:57-61.
76. Zahn S, Kirchner B, Mollenhauer D. Charge Spreading in Deep Eutectic Solvents. ChemPhysChem. 2016;17:3354-8.
77. Ashworth CR, Matthews RP, Welton T, Hunt PA. Doubly ionic hydrogen bond interactions within the choline chloride-urea deep eutectic solvent. Phys Chem Chem Phys. 2016;18:18145-60.
78. Zahn S. Deep eutectic solvents: similia similibus solvuntur? . Phys Chem Chem Phys. 2017;19:4041-7.
79. Wagle DV, Baker GA, Mamontov E. Differential Microscopic Mobility of Components within a Deep Eutectic Solvent. J Phys Chem Lett. 2015;6:2924–8.
80. Preiss UP, Beichel W, Erle AMT, Paulechka YU, Krossing I. Is Universal, Simple Melting Point Prediction Possible? ChemPhysChem. 2011;12:2959 – 72.
81. García G, Aparicio S, Ullah R, Atilhan M. Deep Eutectic Solvents: Physicochemical Properties and Gas Separation Applications. Energy Fuels. 2015;29:2616–44.
82. Alhadid A, Mokrushina L, Minceva M. Design of Deep Eutectic Systems: A Simple Approach for Preselecting Eutectic Mixture Constituents. Molecules. 2020;25:1077.
83. Hammond OS, Bowron DT, Edler KJ. Liquid structure of the choline chloride-urea deep eutectic solvent (reline) from neutron diffraction and atomistic modelling. Green Chem. 2016;18:2736-44.
84. Hammond OS, Edler KJ. Structure and Implications. In: Ramón DJ, Guillena G, editors. Deep Eutectic Solvents: Synthesis, Properties, and Applications: John Wiley & Sons; 2019. p. 25-42.
85. Fetisov EO, Harwood DB, Kuo I-FW, Warrag SEE, Kroon MC, Peters CJ, et al. First-Principles Molecular Dynamics Study of a Deep Eutectic Solvent: Choline Chloride/Urea and Its Mixture with Water. J Phys Chem B. 2018;122:1245–54.
86. Alizadeh V, Malberg F, Padua AAH, Kirchner B. Are There Magic Compositions in Deep Eutectic Solvents? Effects of Composition and Water Content in Choline Chloride/Ethylene Glycol from Ab Initio Molecular Dynamics. J Phys Chem B. 2020;124:7433-43.
87. Malik A, Dhattarwal HS, Kashyap HK. Distinct Solvation Structures of CO2 and SO2 in Reline and Ethaline Deep Eutectic Solvents Revealed by AIMD Simulations. J Phys Chem B. 2021;125:1852-60.
88. Alizadeh V, Esser L, Kirchner B. How is CO2 absorbed into a deep eutectic solvent? J Chem Phys. 2021;154:094503.
89. Abbott AP, Harris RC, Ryder KS, D'Agostino C, Gladden LF, Mantle MD. Glycerol eutectics as sustainable solvent systems. Green Chem. 2011;13:82-90.
90. D'Agostino C, Gladden LF, Mantle MD, Abbott AP, Essa IA, Al-Murshedi AYM, et al. Molecular and ionic diffusion in aqueous – deep eutectic solvent mixtures: probing inter-molecular interactions using PFG NMR. Phys Chem Chem Phys. 2015;17:15297-304.
91. Pandey A, Rai R, Pal M, Pandey S. How polar are choline chloride-based deep eutectic solvents? Phys Chem Chem Phys. 2014;16:1559-68.

92. Pandey A, Pandey S. Solvatochromic Probe Behavior within Choline Chloride-Based Deep Eutectic Solvents: Effect of Temperature and Water. J Phys Chem B. 2014;118:14652–61.
93. Araujo CF, Coutinho JAP, Nolasco MM, Parker SF, Ribeiro-Claro PJA, Rudić S, et al. Inelastic neutron scattering study of reline: shedding light on the hydrogen bonding network of deep eutectic solvents. Phys Chem Chem Phys. 2017;19:17998-8009.
94. Rain MI, Iqbal H, Saha M, Ali MA, Chohan HK, Rahman MS, et al. A comprehensive computational and principal component analysis on various choline chloride-based deep eutectic solvents to reveal their structural and spectroscopic properties. J Chem Phys. 2021;155:044308.
95. Greaves TL, Drummond CJ. Protic Ionic Liquids: Evolving Structure–Property Relationships and Expanding Applications. Chem Rev. 2015;115:11379–448.
96. Fischer SA, Gunlycke D. Analysis of Correlated Dynamics in the Grotthuss Mechanism of Proton Diffusion. J Phys Chem B. 2019;123:5536−44.
97. Ingenmey J, Gehrke S, Kirchner B. How to Harvest Grotthuss Diffusion in Protic Ionic Liquid Electrolyte Systems. ChemSusChem. 2018;11:1900-10.
98. Carrasco-Busturia D, Lysgaard S, Jankowski P, Vegge T, Bhowmik A, García-Lastra JM. Ab initio Molecular Dynamics Investigations of the Speciation and Reactivity of Deep Eutectic Electrolytes in Aluminum Batteries. ChemSusChem. 2021;14:2034-41.
99. Wang J, Wolf RM, Caldwell JW, Kollman PA, Case DA. Development and Testing of a General Amber Force Field. J Comput Chem. 2004;25:1157-74.
100. Mayo SL, Olafson BD, Goddard WA. Dreiding: A Generic Force Field for Molecular Simulations. J Phys Chem. 1990;94:8897-909.
101. Sambasivarao SV, Acevedo O. Development of OPLS-AA Force Field Parameters for 68 Unique Ionic Liquids. J Chem Theory Comput. 2009;5:1038-50.
102. Doherty B, Zhong X, Gathiaka S, Li B, Acevedo O. Revisiting OPLS Force Field Parameters for Ionic Liquid Simulations. J Chem Theory Comput. 2017;13:6131-45.
103. Doherty B, Zhong X, Acevedo O. Virtual Site OPLS Force Field for Imidazolium-Based Ionic Liquids. J Phys Chem B. 2018;122:2962-74.
104. Riniker S. Fixed-Charge Atomistic Force Fields for Molecular Dynamics Simulations in the Condensed Phase: An Overview. J Chem Inf Model. 2018;58:565–78.
105. García G, Atilhan M, Aparicio S. The Impact of Charges in Force Field Parameterization for Molecular Dynamics Simulations of Deep Eutectic Solvents. J Mol Liq. 2015;211:506-14.
106. Breneman CM, Wiberg KB. Determining Atom-centered Monopoles from Molecular Electrostatic Potentials. The Need for High Sampling Density in Formamide Conformational Analysis. J Comput Chem. 1990;11:361–73.
107. Besler BH, Merz Jr. KM, Kollman PA. Atomic charges derived from semiempirical methods. J Comput Chem. 1990;11:431-9.
108. Doherty B, Acevedo O. OPLS Force Field for Choline Chloride-Based Deep Eutectic Solvents. J Phys Chem B. 2018;122:9982-93.
109. Bittner JP, Huang L, Zhang N, Kara S, Jakobtorweihen S. Comparison and Validation of Force Fields for Deep Eutectic Solvents in Combination with Water and Alcohol Dehydrogenase. J Chem Theory Comput. 2021;17:5322–41.
110. Bleiziffer P, Schaller K, Riniker S. Machine Learning of Partial Charges Derived from High-Quality Quantum-Mechanical Calculations. J Chem Inf Model. 2018;58:579–90.

111. Zhong X, Velez C, Acevedo O. Partial Charges Optimized by Genetic Algorithms for Deep Eutectic Solvent Simulations. J Chem Theory Comput. 2021;17:3078–87.
112. Zhong X, Acevedo O. Genetic Algorithm Machine Learning (GAML). v. 1.2, 2021, https://github.com/orlandoacevedo/GAML.
113. Ferreira ESC, Voroshylova IV, Pereira CM, Cordeiro MNDS. Improved Force Field Model for the Deep Eutectic Solvent Ethaline: Reliable Physicochemical Properties. J Phys Chem B. 2016;120:10124–37.
114. Perkins SL, Painter P, Colina CM. Molecular dynamic simulations and vibrational analysis of an ionic liquid analogue. J Phys Chem B. 2013;117:10250-60.
115. Ullah R, Atilhan M, Anaya B, Khraisheh M, García G, ElKhattat A, et al. A detailed study of cholinium chloride and levulinic acid deep eutectic solvent system for CO2 capture via experimental and molecular simulation approaches. Phys Chem Chem Phys. 2015;17:20941-60.
116. Mainberger S, Kindlein M, Bezold F, Elts E, Minceva M, Briesen H. Deep eutectic solvent formation: a structural view using molecular dynamics simulations with classical force fields. Mol Phys. 2017;115:1309-21.
117. Cui K, Yethiraj A, Schmidt JR. Influence of Charge Scaling on the Solvation Properties of Ionic Liquid Solutions. J Phys Chem B. 2019;123:9222–9.
118. Chaumont A, Engler E, Schurhammer R. Is Charge Scaling Really Mandatory when Developing Fixed-Charge Atomistic Force Fields for Deep Eutectic Solvents? J Phys Chem B. 2020;124:7239–50.
119. Kaur S, Sharma S, Kashyap HK. Bulk and interfacial structures of reline deep eutectic solvent: A molecular dynamics study. J Chem Phys. 2017;147:194507.
120. Kaur S, Malik A, Kashyap HK. Anatomy of Microscopic Structure of Ethaline Deep Eutectic Solvent Decoded through Molecular Dynamics Simulations. J Phys Chem B. 2019;123:8291–9.
121. McDaniel JG, Yethiraj A. Influence of Electronic Polarization on the Structure of Ionic Liquids. J Phys Chem Lett. 2018;9:4765–70.
122. Bedrov D, Piquemal J-P, Borodin O, MacKerell Jr. AD, Roux B, Schröder C. Molecular Dynamics Simulations of Ionic Liquids and Electrolytes Using Polarizable Force Fields. Chem Rev. 2019;119:7940–95.
123. McDaniel JG, Schmidt J. Next-Generation Force Fields from Symmetry-Adapted Perturbation Theory. Annu Rev Phys Chem. 2016;67:467−88.
124. Jeong K-j, McDaniel JG, Yethiraj A. Deep Eutectic Solvents: Molecular Simulations with a First-Principles Polarizable Force Field. J Phys Chem B. 2021;125:7177–86.
125. Goloviznina K, Gong Z, Pádua AAH. The CL&Pol polarizable force field for the simulation of ionic liquids and eutectic solvents. WIREs Comput Mol Sci. 2021:e1572.
126. Goloviznina K, Gong Z, Gomes MFC, Pádua AAH. Extension of the CL&Pol Polarizable Force Field to Electrolytes, Protic Ionic Liquids, and Deep Eutectic Solvents. J Chem Theory Comput. 2021;17:1606–17.
127. Sun H, Li Y, Wu X, Li G. Theoretical study on the structures and properties of mixtures of urea and choline chloride. J Mol Model. 2013;19:2433-41.
128. Perkins SL, Painter P, Colina CM. Experimental and Computational Studies of Choline Chloride-Based Deep Eutectic Solvents. J Chem Eng Data. 2014;59:3652-62.

129. Baz J, Held C, Pleiss J, Hansen N. Thermophysical properties of glyceline–water mixtures investigated by molecular modelling. Phys Chem Chem Phys. 2019;21:6467−76.
130. Zhang Y, Poe D, Heroux L, Squire H, Doherty BW, Long Z, et al. Liquid Structure and Transport Properties of the Deep Eutectic Solvent Ethaline. J Phys Chem B. 2020;124:5251-64.
131. Alfurayj I, Fraenza CC, Zhang Y, Pandian R, Spittle S, Hansen B, et al. Solvation Dynamics of Wet Ethaline: Water is the Magic Component. J Phys Chem B. 2021;125:8888–901.
132. Ferreira ESC, Voroshylova IV, Figueiredo NM, Cordeiro MNDS. Molecular dynamic study of alcohol-based deep eutectic solvents. J Chem Phys. 2021;155:064506.
133. Rajbangshi J, Mukherjee K, Biswas R. Heterogeneous Orientational Relaxations and Translation–Rotation Decoupling in (Choline Chloride + Urea) Deep Eutectic Solvents: Investigation through Molecular Dynamics Simulations and Dielectric Relaxation Measurements. J Phys Chem B. 2021;125:5920–36.
134. Triolo A, Celso FL, Brehm M, Lisio VD, Russina O. Liquid structure of a choline chloride-water natural deep eutectic solvent: A molecular dynamics characterization. J Mol Liq. 2021;331:115750.
135. Dawass N, Krüger P, Schnell SK, Simon J-M, Vlugt TJH. Kirkwood-Buff integrals from molecular simulation. Fluid Phase Equilib. 2019;486:21-36.
136. Celebi AT, Dawass N, Moultos OA, Vlugt TJH. How sensitive are physical properties of choline chloride–urea mixtures to composition changes: Molecular dynamics simulations and Kirkwood–Buff theory. J Chem Phys. 2021;154:184502.
137. Shayestehpour O, Zahn S. Molecular Features of Reline and Homologous Deep Eutectic Solvents Contributing to Nonideal Mixing Behavior. J Phys Chem B. 2020;124:7586–97.
138. Migliorati V, D'Angelo P. Deep eutectic solvents: A structural point of view on the role of the anion. Chem Phys Lett. 2021;777:138702.
139. Migliorati V, Sessa F, D'Angelo P. Deep eutectic solvents: A structural point of view on the role of the cation. Chem Phys Lett: X. 2019;2:100001.
140. Salehi HS, Ramdin M, Moultos OA, Vlug TJH. Computing solubility parameters of deep eutectic solvents from Molecular Dynamics simulations. Fluid Ph Equilibria. 2019;497:10-8.
141. Shahbaz K, Mjalli FS, Vakili-Nezhaad G, AlNashef IM, Asadov A, Farid MM. Thermogravimetric measurement of deep eutectic solvents vapor pressure. J Mol Liq. 2016;222:61-6.
142. Ravula S, Larm NE, Mottaleb MA, Heitz MP, Baker GA. Vapor Pressure Mapping of Ionic Liquids and Low-Volatility Fluids Using Graded Isothermal Thermogravimetric Analysis. ChemEngineering. 2019;3:42.
143. Ferreira ESC, Voroshylova IV, Koverga VA, Pereira CM, Cordeiro MNDS. Computational and Experimental Study of Propeline: A Choline Chloride Based Deep Eutectic Solvent. J Mol Liq. 2020;298:111978.
144. Salehi HS, Polat HM, Meyer Fd, Houriez C, Coquelet C, Vlugt TJH, et al. Vapor pressures and vapor phase compositions of choline chloride urea and choline chloride ethylene glycol deep eutectic solvents from molecular simulation. J Chem Phys. 2021;155:114504.

145. D'Agostino C. Hole theory as a prediction tool for Brownian diffusive motion in binary mixtures of liquids. RSC Adv. 2017;7:51864-9.
146. Zhao H, Liang Z-C, Li F. An Improved Model for the Conductivity of Room-Temperature Ionic Liquids Based on Hole Theory. J Mol Liq. 2009;149:55-9.
147. Allen MP, Tildesley DJ. Computer Simulation of Liquids: Oxford University Press; 1989.
148. Pópolo MGD, Voth GA. On the Structure and Dynamics of Ionic Liquids. J Phys Chem B. 2004;108:1744-52.
149. Berkowitz ML. Molecular Simulations of Aqueous Electrolytes: Role of Explicit Inclusion of Charge Transfer into Force Fields. J Phys Chem B. 2021;125:13069–76.
150. Lee AJ, Rick SW. The effects of charge transfer on the properties of liquid water. J Chem Phys. 2011;134:184507.
151. Grimme S, Schreiner PR. Computational Chemistry: The Fate of Current Methods and Future Challenges. Angew Chem Int Ed. 2018;57:4170–6.
152. Sammut C, Webb GI. Encyclopedia of Machine Learning and Data Mining: Springer; 2017.
153. Elton DC, Boukouvalas Z, Fuge MD, Chung PW. Deep learning for molecular design—a review of the state of the art. Mol Syst Des Eng. 2019;4:828-49.
154. Stocker S, Csányi G, Reuter K, Margraf JT. Machine learning in chemical reaction space. Nat Commun. 2020;11:5505.
155. Gómez-Bombarelli R, Wei JN, Duvenaud D, Hernández-Lobato JM, Sánchez-Lengeling B, Sheberla D, et al. Automatic Chemical Design Using a Data-Driven Continuous Representation of Molecules. ACS Cent Sci. 2018;4:268-76.
156. Brockherde F, Vogt L, Li L, Tuckerman ME, Burke K, Müller K-R. Bypassing the Kohn-Sham equations with machine learning. Nat Commun. 2017;8:872.
157. Parmar C, Grossmann P, Bussink J, Lambin P, Aerts HJWL. Machine Learning methods for Quantitative Radiomic Biomarkers. Sci Rep. 2015;5:13087.
158. Balabin RM, Lomakina EI. Support vector machine regression (LS-SVM)—an alternative to artificial neural networks (ANNs) for the analysis of quantum chemistry data? Phys, Chem Chem Phys. 2011;13:11710-8.
159. LeCun Y, Bengio Y, Hinton G. Deep learning. Nature. 2015;521:436-44.
160. Hawkins DM. The Problem of Overfitting. J Chem Inf Comput Sci. 2004;44:1-12.
161. Tetko IV, Livingstone DJ, Luik AI. Neural network studies. 1. Comparison of overfitting and overtraining. J Chem Inf Comput Sci. 1995;35:826–33.
162. Koutsoukos S, Philippi F, Malaret F, Welton T. A review on machine learning algorithms for the ionic liquid chemical space. Chem Sci. 2021;12:6820-43.
163. Shahbaz K, Mjalli FS, HashimI. MA, AlNashef M. Prediction of deep eutectic solvents densities at different temperatures. Thermochim Acta. 2011;515:67–72.
164. Shahbaz K, Baroutian S, Mjalli FS, Hashim MA, AlNashef IM. Densities of ammonium and phosphonium based deep eutectic solvents: Prediction using artificial intelligence and group contribution techniques. Thermochim Acta. 2012;527:59-66.
165. Adeyemi I, Abu-Zahra MRM, AlNashef IM. Physicochemical properties of alkanolamine-choline chloride deep eutectic solvents: Measurements, group contribution and artificial intelligence prediction techniques. J Mol Liq. 2018;256:581–90.
166. Mjalli FS, Shahbaz K, AlNashef IM. Modified Rackett equation for modelling the molar volume of deep eutectic solvents. Thermochim Acta. 2015;614:185-90.

167. Kareem MA, Mjalli FS, Hashim MA, AlNashef IM. Phosphonium-Based Ionic Liquids Analogues and Their Physical Properties. J Chem Eng Data. 2010;55:4632–7.
168. Ghareh Bagh FS, Shahbaz K, Mjalli FS, AlNashef IM, Hashim MA. Electrical conductivity of ammonium and phosphonium based deep eutectic solvents: Measurements and artificial intelligence-based prediction. Fluid Ph Equilibria. 2013;356:30-7.
169. Guo W, Hou Y, Ren S, Tian S, Wu W. Formation of Deep Eutectic Solvents by Phenols and Choline Chloride and Their Physical Properties. J Chem Eng Data. 2013;58:866−72.
170. Yadav A, Pandey S. Densities and Viscosities of (Choline Chloride + Urea) Deep Eutectic Solvent and Its Aqueous Mixtures in the Temperature Range 293.15 K to 363.15 K. J Chem Eng Data. 2014;59:2221-9.
171. Gajardo-Parra NF, Cotroneo-Figueroa VP, Aravena P, Vesovic V, Canales RI. Viscosity of Choline Chloride-Based Deep Eutectic Solvents: Experiments and Modeling. J Chem Eng Data. 2020;65:5581–92.
172. Benguerba Y, Alnashef IM, Erto A, Ernst MBB. A quantitative prediction of the viscosity of amine based DESs usingSs-profile molecular descriptors. J Mol Liq. 2019;1184:357-63.
173. Lemaoui T, Darwish AS, Attoui A, Hatab FA, Hammoudi NEH, Benguerba Y, et al. Predicting the density and viscosity of hydrophobic eutectic solvents: towards the development of sustainable solvents. Green Chem. 2020;22:8511–30.
174. Lemaoui T, Darwish AS, Hammoudi NEH, Hatab FA, Attoui A, Alnashef IM, et al. Prediction of Electrical Conductivity of Deep Eutectic Solvents Using COSMO-RS Sigma Profiles as Molecular Descriptors: A Quantitative Structure–Property Relationship Study. Ind Eng Chem Res. 2020;59:13343–54.
175. Behler J, Parrinello M. Generalized Neural-Network Representation of High-Dimensional Potential-Energy Surfaces. Phys Rev Lett. 2007;98:146401.
176. Behler J. Constructing high-dimensional neural network potentials: A tutorial review. Int J Quantum Chem. 2015;115:1032-50.
177. Bartók AP, Payne MC, Kondor R, Csányi G. Gaussian Approximation Potentials: The Accuracy of Quantum Mechanics, without the Electrons. Phys Rev Lett. 2010;104:136403.
178. Bartók AP, Csányi G. Gaussian approximation potentials: A brief tutorial introduction. Int J Quantum Chem. 2015;115:1051–7.
179. Smith JS, Isayev O, Roitberg AE. ANI-1: an extensible neural network potential with DFT accuracy at force field computational cost. Chem Sci. 2017;8:3192-203.
180. Smith JS, Isayev O, Roitberg AE. A data set of 20 million calculated off-equilibrium conformations for organic molecules. Sci Data. 2017;4:170193.
181. Keith JA, Vassilev-Galindo V, Cheng B, Chmiela S, Gastegger M, Müller K-R, et al. Combining Machine Learning and Computational Chemistry for Predictive Insights Into Chemical Systems. Chem Rev. 2021;121:9816–72.